Supplementary information for Secondary organic aerosol formation from gasoline vehicle emissions in a new mobile environmental reaction chamber

S. M. Platt[1], I. El Haddad[1], A.A. Zardini[2], M. Clairotte[2], C. Astorga[2], R. Wolf[1], J. G. Slowik[1], B. Temime-Roussel[3], N. Marchand[3], I. Ježek[4], L. Drinovec[4], G. Močnik[4], O. Möhler[5], R. Richter[1], P. Barmet[1], F. Bianchi[1], U. Baltensperger[1] and A.S.H. Prévôt[1]

[1] Laboratory of Atmospheric Chemistry, Paul Scherrer Institute (PSI), Villigen, CH-5232, Switzerland

[2] Institute for Energy and transport, Sustainable Transport Unit, EC Joint Research Centre, 21027 Ispra, Italy

[3] Aix-Marseille Université, CNRS, LCE FRE 3416, 13331, Marseille, France

[4] Aerosol d.o.o., Sl-100 Ljubljana, Slovenia

[5] Institute for Meteorology and Climate research, Karlsruhe Institute of Technology, 76021 Karlsruhe, Germany

Correspondence to: andre.prevot@psi.ch

S1 Predicted photolysis rates at -7℃

Photolysis rates at -7°C for several gas phase species calculated using Eq. 3 and Eq. 4 (main text) are given in Table 4 (main text). Minor changes in absorption cross section as a function of temperature ($\sigma(t)$) and quantum yield as a function of temperature ($\Phi(t)$) were accounted for as described in the following sub-sections. For nitrous acid (HONO) and formaldehyde (HCHO), no literature data on how to account for the change in σ and Φ as a function of temperature were found. Therefore the small change in photolysis rates in Table 4 are accounted for by the change in the emission fingerprint between 25°C and -7°C (see Fig. 3A, main text).

S1.1 Nitrogen dioxide (NO_2)

The absorption cross section, σ, of NO_2 as a function of temperature (T) is given by the following parameterisation (DeMore et al., 1997), which was used to estimate $\sigma(-7°C)$:

$$\sigma(t) = \sigma(0°C) + aT \quad , \tag{1}$$

with the parameter *a* tabulated in (DeMore et al., 1997). *Φ(t)* is given in the literature at (Atkinson et al., 2004). An estimation of *Φ(-7°C)* was calculated by interpolating the values given in the literature at 25°C and -29°C (Atkinson et al., 2004).

S1.2 Nitrate (NO_3)

σ(-7°C*)* of NO_3 was estimated by interpolating the values given in the literature at 25°C and -43°C (Atkinson et al., 2004). For the photolysis reaction

$$NO_3 + h\nu \rightarrow NO + O_2 \quad , \tag{2}$$

Φ(t) is unity below 587 nm (Atkinson et al., 2004). For the photolysis pathway

$$NO_3 + h\nu \rightarrow NO_2 + O \quad , \tag{3}$$

and the photolysis pathway in Eq. 2 above 587 nm, *Φ(t)* is given at 25°C and -43°C in the literature (Johnston et al., 1996) and *Φ(-7°C)* was estimated by interpolating *σ(λ)* between these values.

S1.3 Ozone O_3

The effect of temperature *T* on *σ* of O_3 is only small, decreasing by <1% between 25°C and -55°C (Malicet et al., 1995), and was therefore neglected here. For the reaction

$$O_3 + h\nu \rightarrow O(^1D) + O_2 \quad , \tag{4}$$

the main pathway of interest since $O(^1D)$ may react with water to produce OH radicals, *Φ(-7°C)* as a function of wavelength *λ* was calculated using the following expression (Atkinson et al., 2004):

$$\Phi(\lambda T) = \left\{\frac{q1}{q1+q2}\right\} \times A1 \times \exp\left\{-\left(\frac{X1-\lambda}{\omega 1}\right)^4\right\} + \left\{\frac{q2}{q1+q2}\right\} \times A2 \times \left\{\frac{T}{300}\right\}^2 \exp\left\{-\left(\frac{X2-\lambda}{\omega 2}\right)^2\right\} + A3 \times \left\{\frac{T}{300}\right\}^{1.5} \exp\left\{-\left(\frac{X3-\lambda}{\omega 3}\right)^2\right\} + c \quad , \tag{5}$$

where

$$q(i) = \exp\left(\frac{vi}{RT}\right) \quad , \tag{6}$$

where R is the molar gas constant ($8.314\ J\ K^{-1}\ mol^{-1}$), and using $A1$ = 0.8036, $A2$ = 8.9061, $A3$ = 0.1192, $X1$ = 304.225, $X2$ = 314, 957, $X3$ = 310.737,$\omega 1$ = 5.576, $\omega 2$ = 6.601, $\omega 3$ = 2.187, $v1$ = 0, $v2$ = 825.518, and c = 0.0765.

References

Atkinson, R., Baulch, D. L., Cox, R. A., Crowley, J. N., Hampson, R. F., Hynes, R. G., Jenkin, M. E., Rossi, M. J., and Troe, J.: Evaluated kinetic and photochemical data for atmospheric chemistry: Volume I-gas phase reactions of Ox, HOx, NOx and SOx species, Atmospheric Chemistry and Physics, 4, 1461-1738, 2004.

DeMore, W. B., Sander, S. P., Golden, D. M., Hampson, R. F., Kurylo, M. J., Howard, C. J., Ravishankara, A. R., Kolb, C. E., Molina, M. J., and Jet Propulsion Lab, C. I. o. T. P.: Chemical kinetics and photochemical data for use in stratospheric modeling, Jet Propulsion Lab., California Inst. of Tech., Pasadena, CA., 1997.

Johnston, H. S., Davis, H. F., and Lee, Y. T.: NO3 Photolysis product channels: Quantum yields from observed energy thresholds, The Journal of Physical Chemistry, 100, 4713-4723, 1996.

Malicet, J., Daumont, D., Charbonnier, J., Parisse, C., Chakir, A., and Brion, J.: Ozone UV spectroscopy. II. Absorption cross-sections and temperature dependence, Journal of atmospheric chemistry, 21, 263-273, 1995.

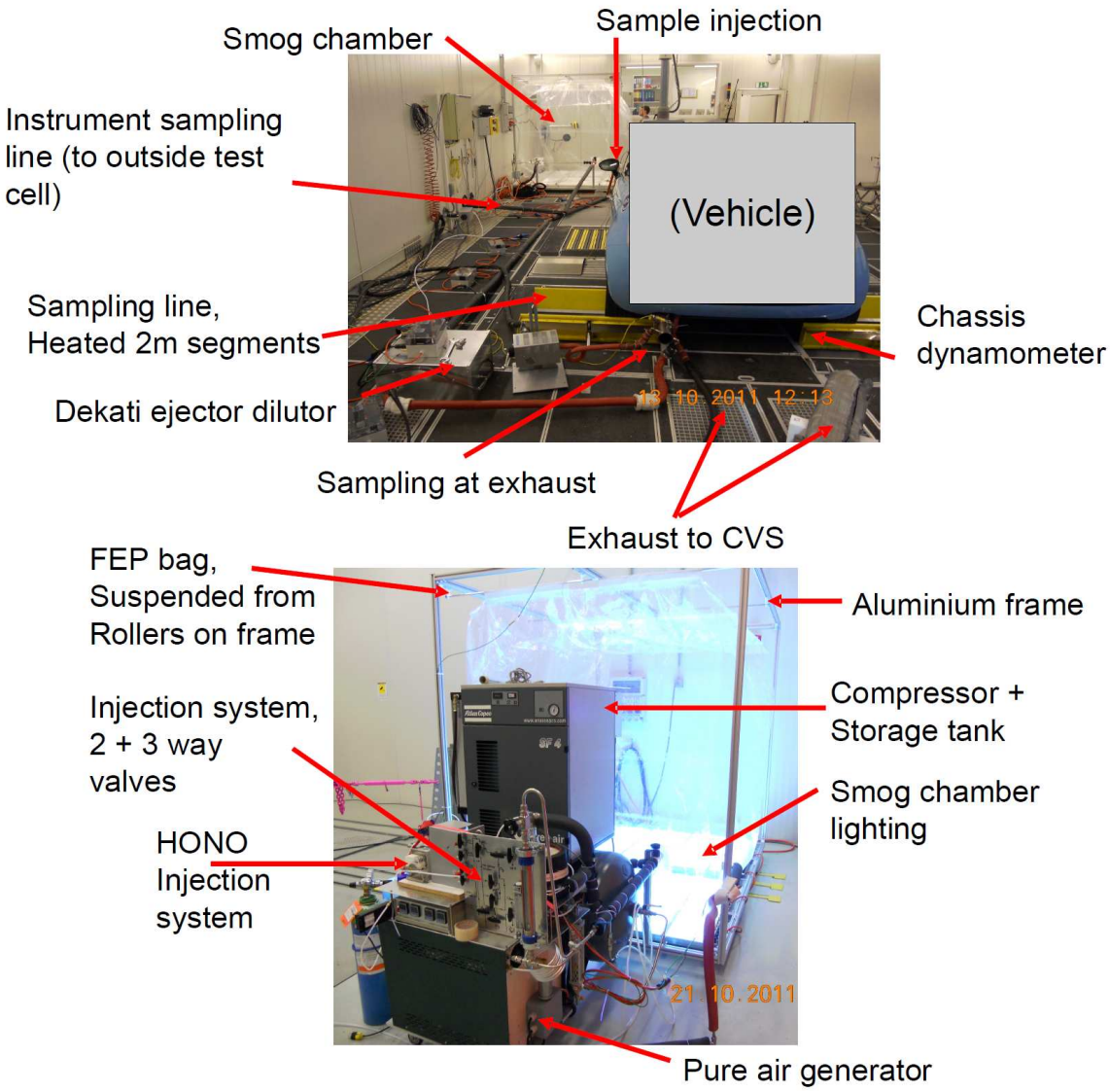

Figure S1: A) Illustrated photograph of the smog chamber and sampling system as set up during sampling of emissions from a gasoline light duty vehicle at the vehicle emissions laboratory (VELA). B) Illustrated photograph of the mobile smog chamber and injection system

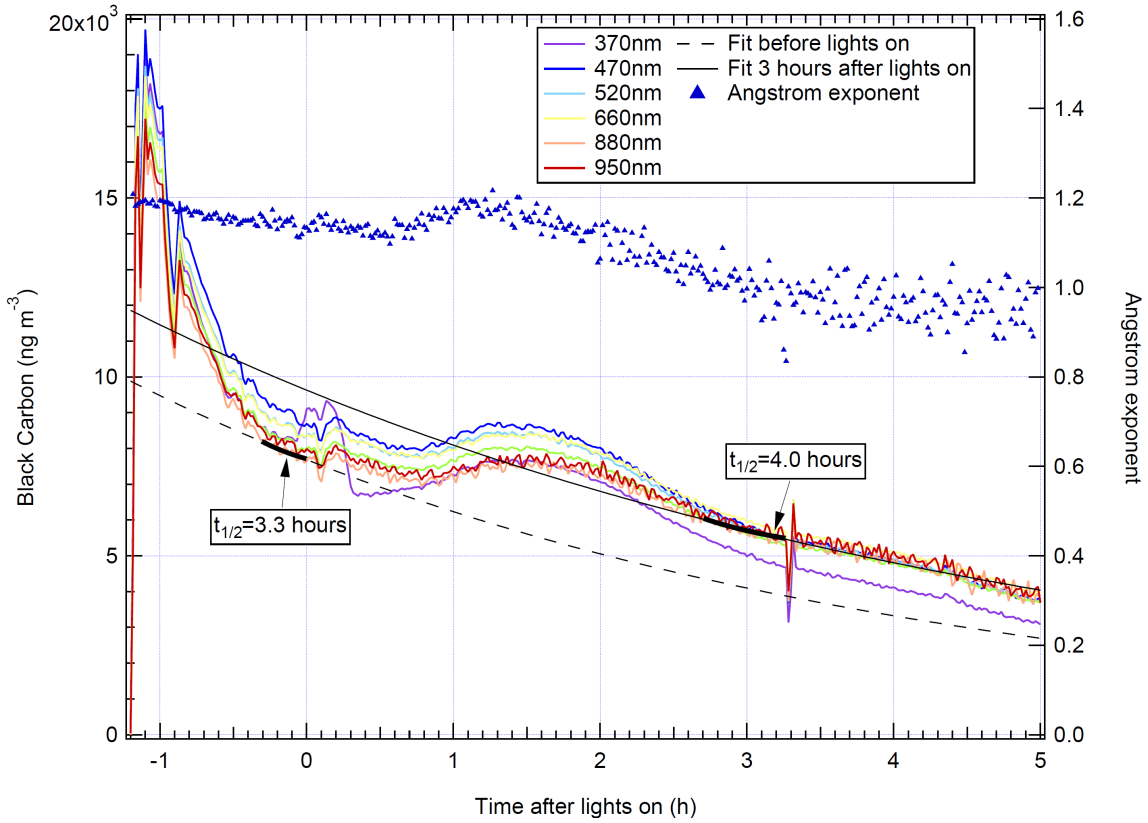

Figure S2: Smog chamber black carbon (BC) concentration measured at different wavelengths using a prototype AE33 aethalometer as a function of time after lights on in the chamber after sampling emissions from a Euro 5 gasoline car. Also shown: particle half lives ($t_{1/2}$) determined from a fit of BC measured at 880nm before lights on (dashed black line) and 3 hours after lights on (solid black line). The fitted region for each curve during each period is highlighted (thick black line) The Angstrom exponent value calculated for each measurement point is shown on the right axis (blue triangles).

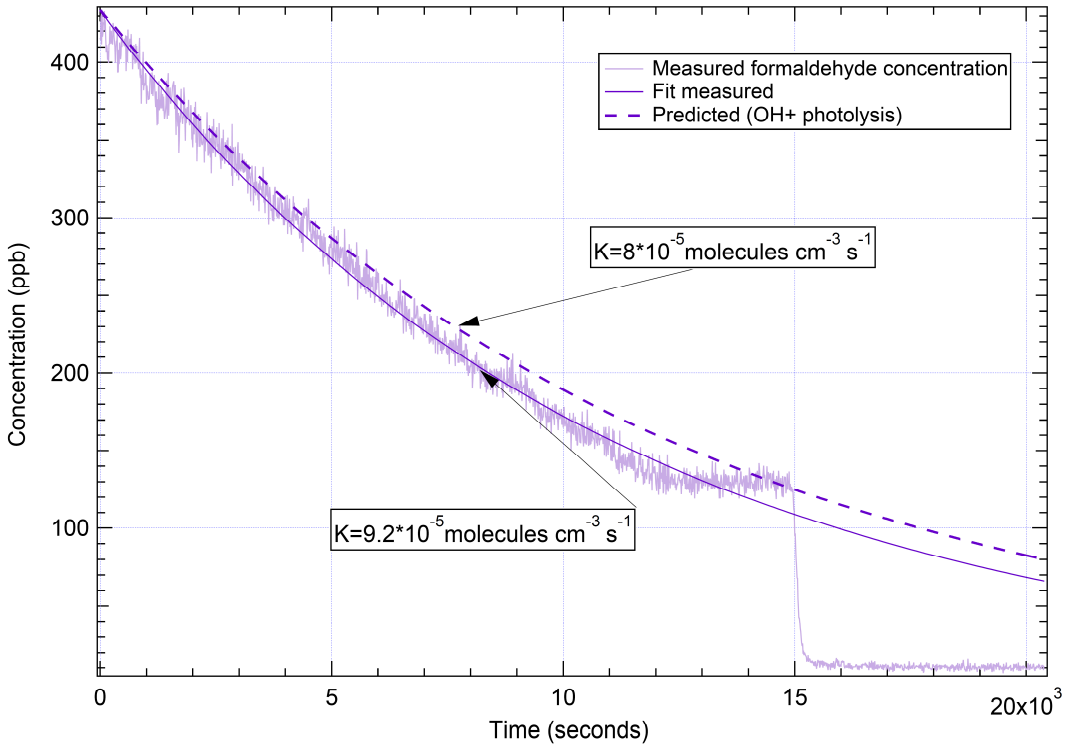

Figure S3: Measured vs. calculated decay of formaldehyde inside the mobile smog chamber under UV lights due to photolysis.

Table S1: Technical details of the Euro 5 gasoline light duty vehicle used in this study

Displacement	Power	Odometer	Gasoline	Fuel system	Weight
875cm3	62.5kW	1376km	CEC RF-02-99 oxy 0.8-1.2	Multipoint port	830 kg

Table S2: Certified properties of the gasoline fuel used in the gasoline light duty vehicle during the driving cycle from which emissions were sampled into the mobile smog chamber

European Commission / Institute for Energy and Transport	**Gasoline CEC-RF-02-99 JRC**	**VELA**

Supplier	**Haltermann Products**
Gasoline Reference	**CEC Legis. Fuel RF-02-99, Ohygen Cont. 0.8-1.2%**
Batch	**QE29513AJ6**

Certificate of analysis

Analysis	Unit'	Result	Limits		Method
		QE29513AJ6	Min	Max	
RON	------	99.20	95.00	------	EN 25164
MON	------	87.50	85.00	------	EN 25163
Density @ 15℃	kg/m3	759.20	------	------	ISO 12185
Density @ 4℃	kg/m3	------	------	------	------
Density @ 15℃	kg/m3	759.20	748.00	762.00	ISO 3675
RVP	kPa	59.80	56.00	60.00	EN 12
Distillation IBP	℃	35.50	24.00	40.00	ISO 3405
Dist.100℃	%vol	51.60	49.00	57.00	ISO 3405
Dist.150℃	%vol	84.80	81.00	87.00	ISO 3405
Distillation FBP	℃	193.50	190.00	215.00	ISO 3405
Dist. Residue	%vol	1.00	------	2.00	ISO 3405
Oxidation Stability	min >	1.2000	------	------	ISO 7536
Olefins	%vol	4.20		10.00	ASTM D1319
Aromatics	%vol	29.60	28.00	40.00	ASTM D1319
Saturates	%vol	61.30	------	------	ASTM D1319
Benzene	%vol	0.20	------	1.00	EN 12177
Oxygenates	%vol	4.90	------	------	EN 1601
tested by subcontractor					
Oxygen Content	% wt	0.9	0.80	1.20	EN 1601
tested by subcontractor					
Hydrogen	% wt	13.16	------	------	ASTM D3343
Carbon	% wt	85.95	------	------	ASTM D3343
C:H Ratio [H=1]	------	6.53	------	------	ASTM D3343